Available online at www.sciencedirect.com

SciVerse ScienceDirect

Energy Procedia 29 (2012) 720 – 730

Energy Procedia

World Hydrogen Energy Conference 2012

Assessment on the long term performance of a $LaNi_5$ based hydrogen storage system

Fusheng Yang[a,b], Xinxin Cao[a], Zaoxiao Zhang[a,b]*, Zewei Bao[a], Zhen Wu[a], Nyallang Nyamsi Serge[a]

[a]*State Key Laboratory of Multiphase Flow in Power Engineering, Xi'an Jiaotong University, Xi'an 710049, P. R.China*
[b]*Suzhou Research Institute, Xi'an Jiaotong University, Suzhou 215123, P. R. China*

Abstract

Metal hydride represents a promising candidate for hydrogen storage, because the technique is essentially safe, compact and flexible. However, the properties of the metal hydride tend to change in repeated hydriding/dehydriding cycles, which will inevitably affect the performance of corresponding hydrogen storage system. The effect is investigated in this paper by numerical simulation using a commercial package COMSOL MULTIPHYSICS 3.5a, and a typical material- $LaNi_5$ is chosen for discussion. Through sensitivity analysis, the influences of variation in key properties over repeated cycles on the charging time of a tank-type storage system, are evaluated and some useful conclusions are drawn.

Keywords: Metal hydride; hydrogen storage system; hydriding/dehydriding cycles; charging time; reaction kinetics.

1. Introduction

Hydrogen, as a clean energy with large energy density, has been paid much attention in recent years. However, its storage and transportation is one key issue to be resolved. The metal hydride is a promising method for the storage of hydrogen due to the large volume capacity, low operation cost and reversible reaction.

Generally, the hydriding/dehydriding reaction can be written as [1]:

$$M + \frac{x}{2} H_2 \leftrightarrow MH_x + \Delta H \qquad (1)$$

* Corresponding author. Tel.: +86-29-8266-0689; fax: +86-29-8266-0689.
E-mail address: zhangzx@mail.xjtu.edu.cn.

1876-6102 © 2012 Published by Elsevier Ltd. Selection and/or peer-review under responsibility of Canadian Hydrogen and Fuel Cell Association.
doi:10.1016/j.egypro.2012.09.084

where M is a certain metal or alloy, and the product MH_x is termed metal hydride (MH). The hydriding/dehydriding reaction needs a suitable reactor, whose design and analysis is a key issue in the relevant applications. Mellouli et al. [2] developed a tank storage system with a spiral-type heat exchanger inserted in the hydride bed. The experimental results showed that the charge/discharge times of the reactor are considerably reduced when heat exchanger is used. Bhouri et al.[3] used the numerical tool to evaluate the influence of fin thickness and the number of heat exchanger tubes on the loading and discharging processes, and the results showed that an optimal number of heat exchanger tubes and bed thickness are important. On the other hand, the long term performance of hydride based storage system, which could be important for evaluating its technical and economical feasibility, has been paid little attention. To evaluate the varying performance of storage system, a numerical model was established here and a typical tank reactor with cooling tubes was chosen for discussion. The variations of many hydride properties over repeated cycles, e.g. permeability, effective thermal conductivity, are considered in the simulation, and the resulting performance variation is analyzed.

2. The variation of MH issue properties

In order to study the long term performance of the reactor, a certain material must be chosen to fill the reactor. Among the hydrogen storage materials, AB_5 type metal hydride material is widely used for the properties of fast kinetics, easy activation and moderate plateau pressure. $LaNi_5$ alloy is the typical representative of the AB_5 type metal hydride material, and its properties have been investigated by many researchers [4-6]. $LaNi_5$ can be used in hydrogen storage, hydrogen compressor and chemical heat pump. In these fields, the metal hydride is expected to work for up to thousands of cycles. The properties of $LaNi_5$ alloy, such as P-C-T equilibrium, reaction kinetics, gas permeability and thermal conductivity, change over cyclic hydriding/dehyderding process. It should be noted that such variation in key properties for $LaNi_5$ is also found for many other AB_5 hydride materials, thus our discussion is of some generality. It has been found that after 300 cycles, the kinetics of $LaNi_{4.75}Al_{0.25}$ and $LaNi_{4.25}Al_{0.75}$ alloy was deteriorated, while those of $LaNi_5$ and $LaNi_{3.8}Al_{1.2}$ alloys was improved [7]. Cheng et al. [8] found that the hydrogen absorption kinetics of $LaNi_{4.25}Al_{0.75}$ alloy degraded significantly beyond 1000 cycles. Murray et al. [9] found that for the $LaNi_5$ alloy the desorption rate increased as the number of cycles increased, but beyond 300 cycles the reaction times became nearly constant. The thermal conductivity of the $LaNi_5$ powder bed is poor (in the range of 0.1–1W/mK) and retards the heat transfer process that occurs with hydriding and dehyderding, and it will become even worse after several cycles. Hahne and Kallweit [10], Isselhorst [11] found that the thermal conductivity varies with hydrogen concentration and pressure, while it will reduce with the hydriding/dehyderding cycles because of the pulverization of the particles. The gas permeability is one of the parameters that affect the kinetics. In some literatures [12], the hydrogen permeability is reported to be $10^{-12}\,m^2$, while in other literatures the hydrogen permeability is $10^{-14}\,m^2$ [13]. Cheng et al. [8] also found that the hysteresis of $LaNi_{4.75}Al_{0.25}$ alloy slightly increases, i.e., the absorption plateau pressures (P_a) systematically increase, while the desorption plateau pressures (P_d) systematically decrease.

Actually, the variations of these metal hydride properties mentioned above are not independent of each other. For example, thermal conductivity, permeability, as well as reaction kinetics all change with the size of MH powders, which is expected to decrease due to pulverization. However, the correlation among these properties is very complex, and there is no proper model available now. Therefore, in this paper our work is confined to the sensitivity analysis, assuming that the other properties are invariant when discussing about the influence of cycling with regard to one property.

3. Mathematical model

3.1. Geometrical model

Linder [14] has set up a cylinder reactor with a capillary tube bundle heat exchanger, showing excellent heat transfer. Here we consider a similar tank–type metal hydride reactor with cooling tube bundles, which is popular in use for hydrogen storage. The physical model is shown in Fig.1, it is a cylinder tank and cooling tubes are uniformly distributed in it. Because of its symmetrical geometry, we just choose a quarter of the reactor as the computation domain for simplicity, as shown in Fig.2.

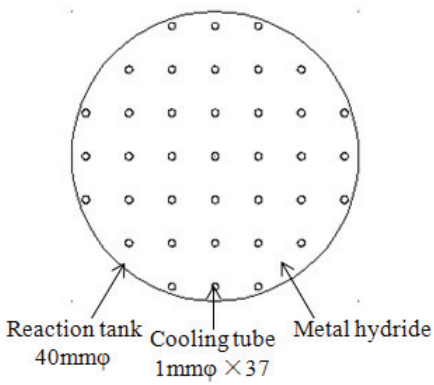

Fig.1 -The surface structure of the tank–type metal hydride reactor with cooling tube bundles

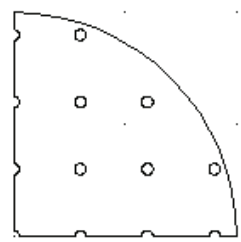

Fig.2 A quarter of the model

3.2. Model formulation

The mathematical model of the cylinder MH reactor was established based on the following assumptions [15]:

- The gas phase is ideal from the thermodynamic view.
- There is no temperature slip between the solid phase and the gas phase, which is also termed “local thermal equilibrium”. This uniform temperature is defined as T_b here.
- The radiative heat transfer can be neglected due to the moderate temperature range in discussion.

The governing equations are described below [15], and some parameters in equations are in Table 1 .

Mass balance equation for hydrogen can be expressed by

$$\frac{\partial \varepsilon_g \rho_g}{\partial t} + \nabla\left(\rho_g \vec{U}\right) = -\dot{m} \qquad (2)$$

where the mass source term is determined by the instantaneous reaction rate, as shown below

$$\dot{m} = \frac{\varepsilon_{MH} \cdot \rho_{MH}}{M_{MH}} \cdot \left[\frac{H}{M}\right]_{sat} \cdot \frac{dX}{dt} \quad (3)$$

The momentum takes the form of the classical Darcy's law

$$\vec{U} = \frac{K}{\mu} \nabla P \quad (4)$$

The energy equation is

$$\frac{\partial \rho_b C_{p,b} T_b}{\partial t} + \nabla\left(\rho_g C_{p,g} \vec{U} T_b\right) = \nabla\left(\lambda_{eff} \nabla T_b\right) + \frac{\dot{m}}{M_g} \cdot \Delta H \quad (5)$$

Where the bulk heat capacity is calculated by the properties of all constituted phases [16], giving

$$\rho_b C_{p,b} = \sum_{i=1} \varepsilon_i \rho_i C_{pi} \quad (6)$$

Reaction kinetics equations are those recommended by Jemni et al. [17],

$$\frac{dX}{dt} = k_a \cdot \exp\left(-\frac{E_a}{R_g T_b}\right) \cdot \ln\left(\frac{P}{P_{e,a}}\right) \cdot (1 - X) \quad (7)$$

In this investigation the plateau slope and hysteresis are explicitly included in the adopted P-C-T equations [18],

$$P_{e,a} = \exp\left(A - \frac{B}{T_b} + \alpha * \tan\left(\pi * (X - 1/2)\right) + \frac{\beta}{2}\right) \quad (8)$$

Table 1 The parameters in the hydrogen absorption kinetics and P-C-T equation.

Kinetic and P-C-T parameters	Values
Rate constant, k (s^{-1})	59.187
Activation energy, E_a (J/mol H_2)	21,179
P-C-T parameter, A (-)	13.44
P-C-T parameter, B (K)	3780
Slope, α(-)	0.038
Hysteresis, β(-)	0.137

3.3. Initial and boundary conditions

The initial reacted condition for hydriding was uniform throughout the reactor. The temperature was equal to that of the inlet fluid, and the system was assumed under the P-C-T equilibrium.

The boundary conditions of MH cylinder tank reactors can be classified into three types [19]: adiabatic wall (or symmetry boundary), heat transfer wall and mass transfer boundary.

For the adiabatic wall (or symmetry boundary):

$$\frac{\partial T_b}{\partial \boldsymbol{n}} = 0 \qquad \frac{\partial p_g}{\partial \boldsymbol{n}} = 0 \tag{9}$$

For the heat transfer wall:

$$-\lambda_{eff} \frac{\partial T_b}{\partial \boldsymbol{n}} = h\left(T_b - T_f\right) \qquad \frac{\partial p_g}{\partial \boldsymbol{n}} = 0 \tag{10}$$

For the mass transfer boundary:

$$\frac{\partial T_b}{\partial \boldsymbol{n}} = 0 \qquad p_g = p_{in} \tag{11}$$

4. Results and discussions

In this work, the charging time of the tank reactor is taken as the index to assess the performance of the hydrogen storage system. The variation of the charging time with increasing cycles was discussed with regard to the P-C-T equilibrium, reaction kinetics, gas permeability and thermal conductivity.

In this investigation, the reactor is filled with $LaNi_5$ alloy, and some physical properties of the material are listed in Table 2 [19]. The operation conditions (initial and boundary conditions) for absorption are given in Table 3.

It should be noted that the given data in Table 2 are just listed as the reference parameters, and will be varied when discussing their effects on the long-term system performance. In the sensitivity investigation, when it is focused on the influence of one property, the others remain unchanged.

Table 2 Physical properties of material (powders) and data used in the simulation

Physical properties	Metal ($LaNi_5$)	Hydrogen
Density, ρ, kg/m^3	8400	—
Specific heat, C_p, J/Kg K	419	—
Effective thermal conductivity, λ_{eff}, W/m K	1.0	—
Permeability, K, m^2	1.0×10^{-12}	—
Reaction enthalpy, ΔH, J/mol	3.01×10^{4}	—
Porosity, ε	0.5	—
Universal gas constant, R_g, J/mol K	—	8.314

Table 3 The operation conditions for hydrogen absorption

Operation parameter	Reference values
External pressure, P_{ex} (MPa)	0.8[20]
Initial reacted fraction, X (—)	0.1
Initial bed temperature, T_b (K)	293
Convective heat transfer coefficient, h (W/(m^2 K))	1500
Fluid inlet temperature, T_f(K)	293

4.1. The effect of the gas permeability

The gas permeability is a function of the particle diameter and porosity of the MH bed, described as:

$$K = \frac{d^2 \times \varepsilon_p^{\ 3}}{180 \times \left(1 - \varepsilon_p\right)^2} \tag{12}$$

Where K is the gas permeability, d is the particle diameter and ε_p is the porosity of the MH bed. Due to the particle pulverization and self-compact phenomenon in the process of hydriding/dehydriding cycles, the gas permeability K will decrease gradually. Therefore, this paper choose 10^{-12}, 10^{-13} and 10^{-14} as the permeability values with increasing cycles, and the simulation results are shown in Fig. 3.

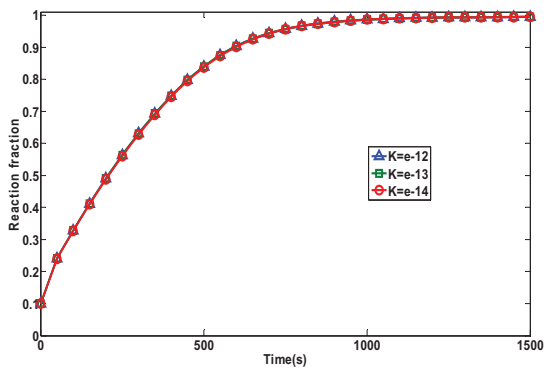

Fig. 3 The kinetics of the $LaNi_5$ at different permeability

An identical charging time of 593s for three different permeabilities are found from Fig. 3, showing that the changes of the gas permeability with cycles basically have little influence on the hydriding reaction rate. The discussion is also extended to varying operation conditions (external pressure changes from 0.6 to 1.2MPa, convective heat transfer coefficient changes from 1000 to 2500W/mK), and similar conclusion can be drawn. Since K is related to the mass transfer, the insensitivity of system performance to permeability suggests that in the coupling hydriding process, mass transfer is not the controlling step.

4.2. The effect of the thermal conductivity

According to Hahne and Kallweit [10], during the first tens of cycles a minor decrease (from 1.0 to 0.65 W/mK at 1.0MPa) in the effective thermal conductivity was observed for the $LaNi_{4.7}Al_{0.3}$ alloy, which has similar particle size decay behavior to $LaNi_5$ in this investigation. Therefore, in the simulation the thermal conductivity values from 1 to 0.6 W/mK are chosen. The Figs. 4-6 show the calculation results.

The results in Fig. 4 illustrate that the deterioration of the thermal conductivity with cycles will lead to remarkable degradation of the performance of the hydrogen storage system. The reaction rate gets slower when λ_{eff} decreases with hydriding/dehydriding cycles, and thus the charging time gets longer.

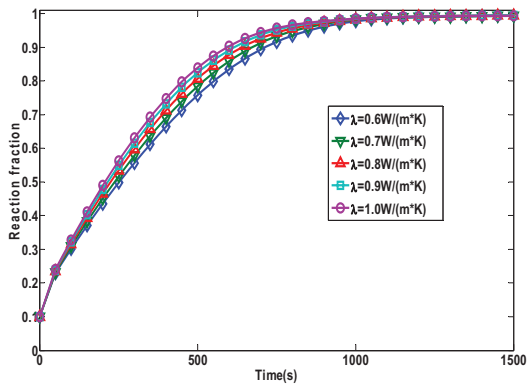

Fig. 4 The kinetics of $LaNi_5$ at different thermal conductivity of reaction bed with cycles

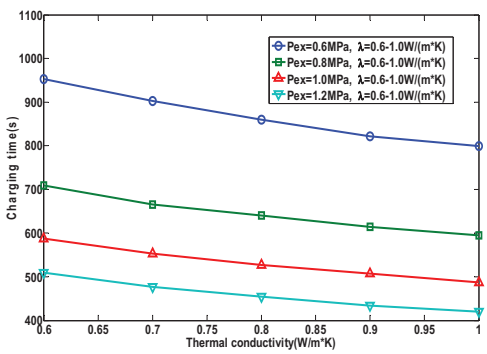

Fig. 5 The charging time at different external pressure within the same range of the thermal conductivity according to different cycle times

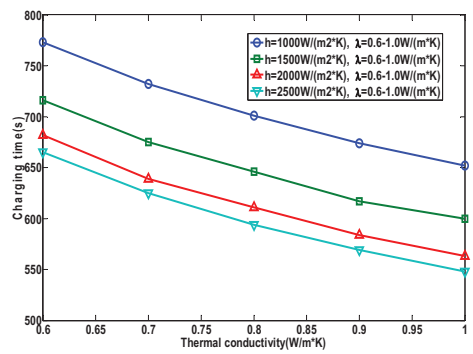

Fig. 6 The charging time at different convective heat transfer coefficient within the same range of the thermal conductivity according to different cycle times

The influence of the thermal conductivity decay on the performance of the hydrogen storage system also depends on operation parameters, such as external pressure and convective heat transfer coefficient. As shown in Fig.5, at an external pressure of 0.6MPa, the thermal conductivity decay causes the charging time to increase by 19%. On the other hand, at an external pressure of 1.2MPa, the charging time will experience a slightly larger extension by 21% due to the same reason.

From Fig. 6, it is found that at a heat transfer coefficient of 1000 W/m^2 K, the thermal conductivity decay results in an increase of charging time by 18%. When the convective heat transfer coefficient increases up to 2500 W/m^2 K, the charging time will be prolonged by 21% due to the decay in thermal conductivity with cycling. Therefore, it can be said when enhanced external transfer condition is provided, the negative effect of thermal conductivity decay on system performance will be more severe.

In summary, it can be concluded that the decay of thermal conductivity with cycling leads to notable deterioration in the performance of the $LaNi_5$ based hydrogen storage system, especially when the operation conditions allow fast reaction kinetics. Therefore, measures should be taken to increase the thermal conductivity and make it more stable with cycles, such as filling Al foam in the bed, using copper foil or making metal hydride compacts.

4.3. The effect of the P-C-T properties

Han et al. conducted an experimental study on the PCT properties of $LaNi_5$ alloy [21], in which they found that the slope of the plateau region is pronounced after 932 hydriding/dehydriding cycles. In this paper data points are chosen from their report for linear fitting, finally the slope of the plateau region and the hysteresis were obtained, as shown in Table 4. These results are used in the simulation.

Table 4 The change of the P-C-T hydriding plateau slope with cycling

	Initial cycle	400 cycles	932 cycles	1510 cycles
Slope α	0.0252	0.0546	0.0728	0.1288
Hysteresis β	0.1931	0.1527	0.2341	0.2286

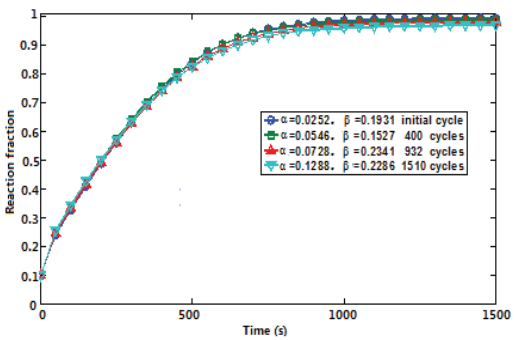

Fig. 7 The kinetics of the $LaNi_5$ considering the slope changes of the P-C-T plateau with cycling.

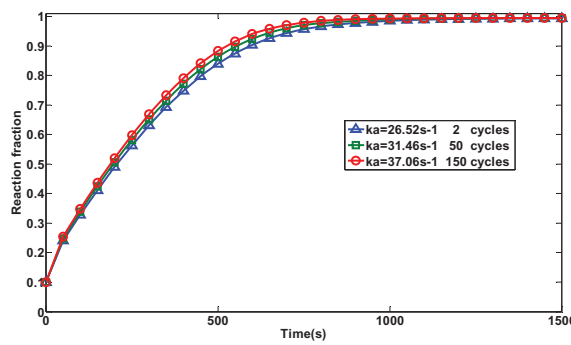

Fig. 8 The hydrogen hydriding reaction rate of the $LaNi_5$ at 293K after cycles

Figure 7 shows the hydriding reaction rate considering the slope and hysteresis change with cycling. It can be seen that the variation in reaction rate is insignificant. The charging times for a sample to absorb 90% of its maximum hydrogen capacity are 590, 592, 620 and 642s for 1, 400, 932 and 1510 cycles. Due to the increasing slope and hysteresis with cycles, the reaction driving force in Eq. (7) tends to decrease,

resulting in the slowing down of hydriding reaction. In a word, marginal deterioration in the performance of hydrogen storage system is predicted over repeated cycles, owing to the varying P-C-T properties.

4.4. The effect of the reaction kinetics

Cheng et al. [22] found that the hydriding reaction kinetics of $LaNi_5$ is improved with the increase of hydriding/dehydriding cycles. Many data points are chosen from their article, and the reaction rate constant k described in equation (12) is obtained by curve fitting. When the cycle number is 2, 50 and 150, the corresponding value of k is 0.0161, 0.0191 and 0.0225, respectively.

$$\frac{dX}{dt} = k\left(1 - X\right) \tag{13}$$

Here the parameter k can be further expressed as

$$k = k_a \cdot \exp\left(-\frac{E_a}{R_g T_b}\right) \cdot \ln\left(\frac{P}{P_{e,a}}\right) \tag{14}$$

In this work, E_a is assumed to be constant, as shown in Table 1. From the gas pressure and bed temperature [22], the parameter k_a is calculated. The three values are 26.52, 31.46 and 37.06s^{-1}, corresponding to 2, 50 and 150 cycles, respectively. The simulation results using the k_a values obtained above are shown in Fig. 8. As can be found in the figure, after multiple hydriding/dehydriding cycles the hydriding reaction rate is improved. The charging times for a sample to absorb 90% of its maximum hydrogen capacity are 590, 549 and 522s for the 2, 50 and 150 cycles, respectively. Therefore, from the simulation results it can be concluded that the performance of the $LaNi_5$ based hydrogen storage system will be improved with the hydriding/dehydriding cycles, concerning the enhanced hydriding kinetics.

.

5. Conclusion

The effect of the properties changes of $LaNi_5$ alloy with cycling on the performance of a hydrogen storage system is studied, and the following conclusions can be drawn:

- The changes of the gas permeability with repeated hydriding/dehydriding cycles basically have no influence on the performance of $LaNi_5$ based hydrogen storage system.
- The decay in thermal conductivity with cycles has a big influence on the performance of the hydrogen storage system. When the external pressure and the convective heat transfer coefficient increases, the abovementioned effect gets more significant.
- The change of the P-C-T properties with cycling, more specifically the increasing slope and hysteresis, leads to slightly deteriorated performance of the $LaNi_5$ based hydrogen storage system.
- Due to the accelerated hydriding kinetics with the cycles, the performance of the $LaNi_5$ based hydrogen storage system will be improved noticeably.

Acknowledgements

The financial support from the National Natural Science Foundation of China (No.51106118), the Ph. D Program Foundation of Chinese Education Ministry (No.20100201110007), the Application

Fundamentals Research Program of Suzhou City (No.SYG201019) are greatly acknowledged.

References

[1] Yang FS, Zhang ZX, Wang GX, Bao ZW, Diniz da Costa J C, Rudolph V. Numerical study of a metal hydride heat transformer for low-grade heat recovery simulation of a MH heat transformer. Applied Thermal Engineering. 2011; **31**: 2749-56.

[2] Mellouli S, Askri F, Dhaou H, Jemni A, Ben Nasrallah S. A novel design of a heat exchanger for a metal hydride reactor. Int J Hydrogen Energy 2007; **32**:3501–7.

[3] Bhouri M, Goyette J, Hardy BJ, Anton DL. Sensitivity study of alanate hydride storage system. Int J Hydrogen Energy. 2011; **36**: 621-33.

[4] Nahm KS, Kim WY, Hong SP, Lee WY. The reaction kinetics of hydrogen storage in $LaNi_5$. Int J Hydrogen Energy. 1992; **17**: 333-38.

[5] Yu XN, Schlapbach L. Surface properties of chemically prepared $LaNi_5$ and its oxidation and poisoning by O_2 and CO. Int J Hydrogen Energy. 1988; **13**: 429-32.

[6] Diaz H, Percheron-guegan A, Achard JC, Chatillon C, Mathieu JC. Thermodynamic and structural properties of $LaNi_{5-y}Al_y$ compounds and their related hydrides. Int J Hydrogen Energy. 1979; **4**: 445-54.

[7] Cheng HH. Special hydrogen storage materials and the measurement apparatus. Ph.D. dissertation of Institute of Metal Research, Chinese Academic of Sciences, 2007.

[8] Cheng HH, Yang HG, Li SL, Deng XX, Chen DM, Yang K. Effect of hydrogen absorption/desorption cycling on hydrogen storage performance of $LaNi_{4.25}Al_{0.75}$. J Alloys Compd. 2008; **453**: 448-52.

[9] Murray J, Miller H, Bird P, Goudy AJ. The effect of particle size and surface composition on the reaction rates of some hydrogen storage alloys. J Alloys Compd. 1995; **231**: 841-45.

[10] Hahne E, Kallweit J. Thermal conductivity of metal hydride materials for storage of hydrogen: experimental investigation. Int J Hydrogen Energy. 1998; **23**: 107–14.

[11] Isselhorst A. Heat and mass transfer in coupled hydride reaction beds. J Alloys Compd 1995; **231**: 871-9.

[12] Ben Nasrallah S, Jemni A. Heat and mass transfer models in metal-hydrogen reactor. Int J Hydrogen Energy. 1997; **22**: 67-76.

[13] Lloyd GM, Razani A, Feldman Jr KT. Proceedings of ASME International Mechanical Engineering Congress and Exposition. 1995; AES-34: 205.

[14] Linder M, Mertz R, Laurien E. Experimental analysis of fast metal hydride reaction bed dynamics. Int J Hydrogen Energy. 2010; **35**: 8755-61.

[15] Yang FS, Wang GX, Zhang ZX, Rudolph V. Investigation on the influences of heat transfer enhancement measures in a metal hydride heat pump. Int J Hydrogen Energy. 2010; **35**: 9725-35.

[16] Laurencelle A, Goyette J. Simulation of heat transfer in a metal hydride reactor with aluminium foam. Int J Hydrogen Energy. 2007; **32**: 2957-64.

[17] Jemini A, Ben Nasrallah S. Study of two-dimensional heat and mass transfer during absorption in a metal-hydrogen reactor. Int J Hydrogen Energy. 1995; **20**: 43-52.

[18] Nishizaki T, Miyamoto K, Yoshida K. Coefficients of performance of hydride heat pumps. J Less-Common Met. 1983; **89**: 559-66.

[19] Yang FS, Meng XY, Deng JQ, Wang YQ, Zhang ZX. Identifying heat and mass transfer characteristics of metal hydride reactor during adsorption: improved formulation about parameter analysis. Int J Hydrogen Energy. 2009; **34**: 1852-61.

[20] Askri F, Jemni A, Ben Nasrallah S. Study of two-dimensional and dynamic heat and mass transfer in a metal-hydrogen reactor. Int J Hydrogen Energy 2003; **28**: 537-57.

[21] Han JI, Lee JY. An investigation of the intrinsic degradation mechanism of $LaNi_5$ by thermal desoprtion technique. Int J Hydrogen Energy. 1988; **13**: 577-81.

[22] Cheng HH, Chen DM, Yang K. New type property measuring apparatus and applications for hydrogen storage material. Rare metal materials and engineering (in Chinese). 2007; **36**: 78-81.